Multirhythmicity generated by slow variable diffusion in a ring of relaxation oscillators and noise-induced abnormal interspike variability

E. I. Volkov and D. V. Volkov
Department of Theoretical Physics, Lebedev Physical Institute, Leninskii 53, Moscow, Russia
(Received 9 April 2001; revised manuscript received 22 January 2002; published 10 April 2002)

The deterministic and noise-dependent dynamics of a ring of three Ohmically coupled electronic relaxation oscillators are considered by means of numerical simulations. Each isolated oscillator is described by a set of two ordinary differential equations with very different characteristic times. The emergence of the limit cycle via the Hopf bifurcation results from the N-shaped current-versus-voltage characteristic of the nonlinear resistor. The phase diagram is calculated for a ring of three such oscillators in the presence of small detuning. Special attention is focused on two parameter areas, one near a transition to the homogeneous and the other near the inhomogeneous stable steady state. Along with other nontrivial limit cycles, essentially asymmetrical limit cycles termed dynamic traps may arise in these two areas. A dynamic trap is a regime in which one or two oscillators do not perform full-amplitude oscillations and, correspondingly, do not generate spikes. The interspike interval (ISI) distribution in the presence of noise is calculated as a function of the coupling strength in both areas of the parameter plane. The distributions are extremely polymodal near the homogeneous steady state even if the in-phase limit cycle is dominating. The origins of this abnormal enhancement of ISI variability are discussed in detail. A similar analysis shows that nontrivial periodic attractors are observable in the vicinity of the inhomogeneous stable steady states only if the level of noise is relatively low. In this case, the dominance of the in-phase limit cycle basin results in an almost unimodal distribution of interspike intervals.

DOI: 10.1103/PhysRevE.65.046232 PACS number(s): 05.45.−a, 05.40.−a

I. INTRODUCTION

Ensembles of coupled oscillators have been used for a long time as models of biological processes. For example, in [1], a population consisting of a large number of almost identical oscillators, each of which is weakly coupled to all the others, is considered to be a model for the source of circadian rhythms (see also [2,3]). Long chains of almost linear oscillators are used to imitate the contraction waves of the small intestine [4]. Small ensembles of four, six, or eight cells have become popular in explaining the gaits of legged animals [5–7].

The dynamics of locally coupled ''theoretical'' oscillators [8–10], neurons [11] (see [12] for recent examples), and electronic [13,14], and chemical [15–20] oscillators is also being studied extensively in order to reveal as many collective modes as possible in systems consisting of identical or nearly identical elements. Comprehensive analysis of the dynamics of ensembles of relaxation oscillators has revealed that several out-of-phase modes may be stable in a broad parameter range if the stiffness of individual oscillators is high and slow (recovery) variable exchange dominates [21,22].

Although the dynamics of systems composed of relaxation oscillators is difficult to analyze analytically or numerically, relaxation oscillators, in our opinion, describe the reality more adequately, because the trajectories of many biological and chemical oscillators are far from being harmonic [23]. In addition, it is known from early work [24] and from recent investigations of oscillators coupled via ''fast threshold modulation'' [25] that arrays of relaxation oscillators are more suitable candidates for control systems than nonrelaxation ones because the time required for the latter to become synchronized is much longer.

A system was recently studied [26] that consisted of three almost identical electronic oscillators coupled via resistors. This type of coupling implies linear diffusion of only slow variables (voltage in this specific case), which enhances the phase differences between the phase points located on the different branches of the N-shaped nullcline of the fast variable. However, this exchange does not affect the stability of the homogeneous state (in-phase oscillations) in ensembles of two-dimensional identical oscillators. The largest volume of the parameter space in systems of three identical oscillators with cyclic boundary conditions is occupied by so-called rotating waves (RWs) of various types. Rotating waves are periodic solutions with the same wave form $X_i(t)$ for each oscillator, and the phase shifts by one-third of the period between adjacent oscillators in a chain. A simple rotating wave contains one spike of the fast variable per period. However, if stiff oscillators are strongly coupled, more intricate RWs are also stable in certain parts of the parameter space. The second generic solution is an antiphase attractor, which is characterized by the in-phase oscillation of two elements phase-shifted by half a period relative to the third one. The existence of these attractors does not depend on the choice of the model for the nonlinear oscillator [10]. They have been demonstrated in experiments with chemical [19] and electronic [14] systems.

As shown both numerically and experimentally [26], a subtle increase in the period of one of the oscillators is responsible for the emergence of a large region in the parameter space where a ring of coupled oscillators loses amplitude symmetry. Specifically, full-amplitude oscillations become inhibited in the retarded oscillator. Asymmetrical periodic attractors in which slow variable exchange causes at least one oscillator to stop generating spikes rhythmically will be

referred to below as ''dynamic traps'' (DTs). Two models, one describing two identical neurons [27] and the other three-membrane timers [28], have also been shown to possess stable highly asymmetrical solutions. However, the areas of their existence shrink rapidly with increasing stiffness of the elements. For our set of parameters of the electronic oscillator, such attractors are unobservable in the absence of detuning. We demonstrate here that a minor modification of the experimental setup used in [26] and subtle detuning in the periods of oscillations of individual units may result in the emergence of DTs in the vicinity of bifurcations from oscillations not only to the homogeneous but also to the inhomogeneous steady states.

With such a diverse set of stable attractors, it is of particular importance to examine the role of noise in the generation of collective behaviors. Therefore, in this study, we continue to numerically analyze the dynamic properties of a ring of three slightly detuned electronic oscillators in the presence of noncorrelated noise. Specifically, we consider the case when the internal parameters of individual oscillators determine the extent of detuning without affecting the coupling strength. In the presence of noise, the interspike interval (ISI) distributions for full-amplitude oscillations are convenient characteristics of the dynamic behavior of the system. It is usually expected that the relative peak amplitudes in the ISI histograms will reflect the sizes of basins of coexisting stable attractors and that the peaks' positions are determined by the periods of the limit cycles and/or by the characteristic times of transitions between the attractors.

Detailed analysis of wave forms reveals the mechanisms giving rise to the peaks in the ISI distributions in the ranges of existence of periodic attractors and in the range of existence of a unique in-phase regime near the transition to the homogeneous steady state. We demonstrate how noise interaction with intense slow variable exchange generates abnormally long ISIs even for identical oscillators, which can move only in phase or in antiphase in the absence of noise. The relationships are discussed between long ISIs and deterministic detuning-dependent attractors, including DTs. As a counterexample to this unusual spiking regime, we describe the expected noise-induced spiking behavior near the transition to inhomogeneous steady states, where both a DT and a RW exist, but the ISI distributions remain unimodal because of the strong dominance of the in-phase limit cycle.

The paper is organized as follows. Sections II and III present a brief description of the isolated oscillator and the numerical methods, respectively. The deterministic dynamics is examined in Sec. IV by constructing the phase diagram for three identical oscillators; their detuning is described in Sec. IV A. Thereafter, we consider the evolution of the basic modes in the presence of small detuning (Sec. IV B) and demonstrate the existence of a DT near the homogeneous steady state (Sec. IV C). The detuning-dependent DTs and the phase diagram near the stable inhomogeneous steady states are investigated in Sec. V. Section VI presents a ''microscopic'' analysis of the main peaks in the ISI distributions. The preliminary results of this work have been briefly reported elsewhere [29].

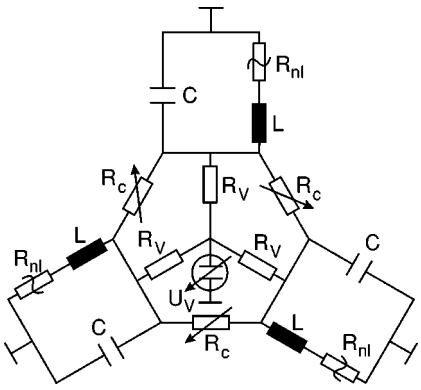

FIG. 1. Scheme of the experimental setup used to numerically analyze its dynamic behavior. The setup consists of three nonlinearity (R_{nl}) -containing oscillators connected in parallel. Resistors R_V are different; all other parameters are homogeneous: $C=215$ μF and $L=33$ mH. The supply voltage U_V and the coupling resistors R_c are the control parameters; the variables U_i in the model equations are the voltage drops at capacitors.

II. ELECTRONIC OSCILLATOR

We chose to study numerically a ring of three electronic oscillators coupled through Ohmic resistors (Fig. 1). Simulations were performed for the same nullcline and relaxation parameters that were used in [26]. As seen in the figure, an individual electronic oscillator is an LC circuit containing a nonlinear resistor R_{nl}, which accounts for the N-shaped current-versus-voltage characteristic and, hence, for the N-shaped nullcline in the set of differential equations corresponding to this scheme (Fig. 1):

$$L\frac{dI_i}{dt}=U_i-S(I_i), \tag{1}$$

$$C\frac{dU_i}{dt}=\frac{U_V+U_i}{R_{Vi}}-I_i+\frac{U_{i-1}-2U_i+U_{i+1}}{R_c}, \tag{2}$$

where $i=1,2,3 \pmod 3$.

In its turn, a nonlinear resistor is a separate electronic device. Its current-versus-voltage characteristic has been determined experimentally in a previous study (see [26] for details). The individual oscillator's phase portrait and the time series of the dynamic variables are shown in Fig. 2. As clearly seen in this figure, the oscillators with the parameters chosen are stiff.

The oscillators are made nonidentical by setting their resistances R_V (rather than capacitances, as in the previous study [26]) to slightly different values. We chose the latter based on the dependence of the period on R_V for different U_V values (see Sec. IV A). Note that, with this approach, we have the period of the isolated oscillator independent of the parameters that control the coupling strength.

III. METHODS

Equations (1) and (2) were solved using general numerical methods. For not very stiff equations, we implemented an explicit fourth-order (double-precision) Runge-Kutta routine

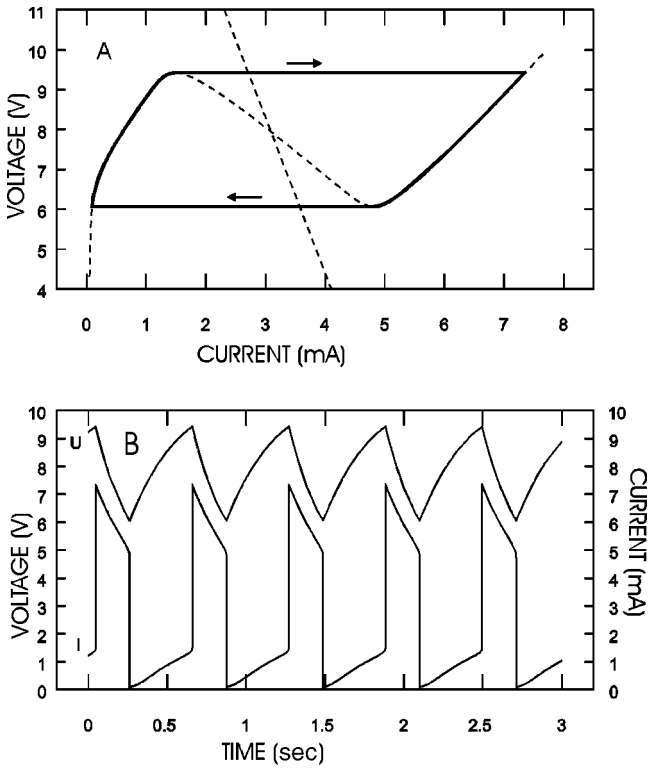

FIG. 2. (a) Phase portrait of the isolated electronic oscillator and (b) time series of its dynamic variables (slow U and fast I) for $U_V=20$ V. The limit cycle and main nullclines are indicated by solid and dashed lines, respectively.

with step size control (subroutine named DRKGS from the SSP library). If the stiffness was large, implicit integrators were used of which RADAU5 proved most efficient. To be confident that the results obtained are not numerical artifacts or long-lived transients, we tested whether they varied depending on the method used and/or on the accuracy set in computations. The algorithms were constructed for seeking and identifying the attractors by randomly varying the initial points and observing the dynamics of changes in the ISIs of each oscillator during the settling of the system on the attractor (see [22] for more details).

IV. DETERMINISTIC DYNAMICS

A. The system of identical oscillators and the method for its detuning

Even for identical oscillators, quite complex solutions exist in the model (1), (2) in various areas of the parameter plane (Fig. 3 here or Fig. 4 in [26]). In addition to the in-phase solution (which is stable everywhere in the parameter plane), Fig. 3 depicts the areas occupied by stable rotating waves of various types. Along with a simple RW whose period contains only one interspike interval, we observed regimes in which two, five, and seven interspike intervals per one period were present (RW2, RW5, and RW7, respectively). A large area of the parameter plane is occupied by the stable antiphase attractor marked 1/2 in Fig. 3.

Along with periodic attractors, the phase diagram shows the boundaries of stable inhomogeneous steady states SS I and SS II ("amplitude death" in other terminology; see the caption to Fig. 3). As in [26], the solutions observed for identical oscillators will be referred to as "basic" modes.

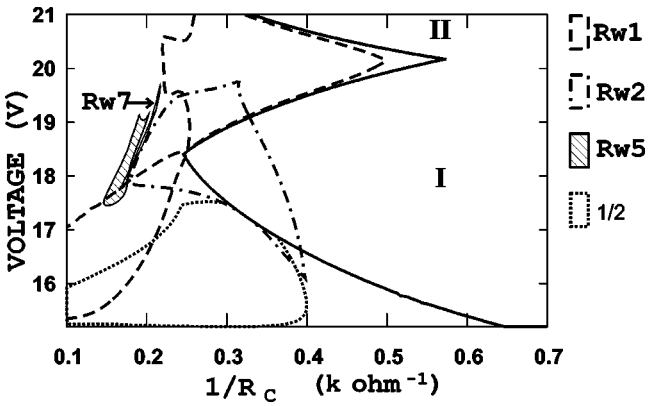

FIG. 3. Part of the phase diagram of basic periodic attractors for identical oscillators. Different types of rotating wave are designated as RW1, RW2, RW5, and RW7; 1/2 indicates the antiphase limit cycle. The attractors are stable inside the closed regions depicted by the appropriate lines. Note that there are two regions where RW1 is stable. The boundaries of the stable inhomogeneous steady states ("amplitude deaths") SS I and SS II are indicated by solid lines. In region I, the steady states $U_{1,2}$ are large and $I_{1,2}$ small, while U_3 is small and I_3 large. In region II, one oscillator has large U, while two others have small U_i.

Inequality of limit cycles may be generated by changes in one or more control parameters. The differences between the periods of uncoupled oscillators may serve as an index of detuning. As mentioned above, variation in the R_{V_i} values, which determine the slope of one of the main isoclines $U_i = R_{V_i} I_i - U_V$, will be used to study the role of detuning in the generation of collective modes.

The period of a free oscillator is a nonlinear function of the control parameters R_V and U_V (see Fig. 4). Even if the oscillators are only slightly different with respect to R_V, their periods may vary considerably, depending on the parameter U_V. We confine ourselves to examining oscillators that differ in the free period by no more than 1% to 3%.

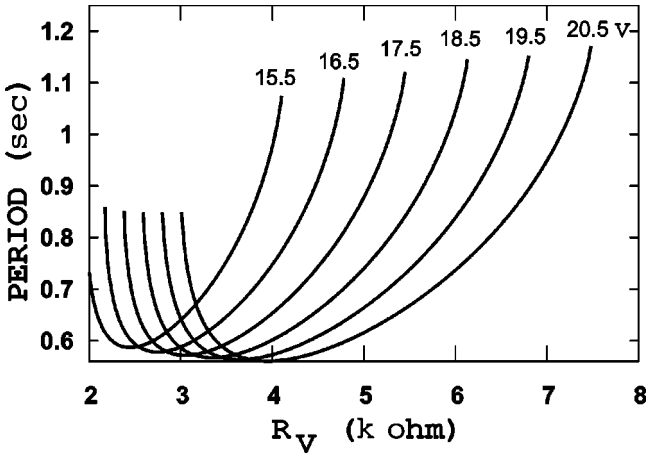

FIG. 4. Dependences of free periods on parameter R_V for different U_V.

This detuning index is so small that, with R_{V_i} fixed, it is not feasible to keep it at this level throughout the U_V range where the limit cycle is stable. Therefore, we will search for dynamic traps in two separate areas of the phase diagram that are most promising in this respect. One of these two areas is located near the boundary of the homogeneous steady state: $U_V=15.2$ V–16.5 V. Formally, this steady state is not homogeneous and not unique if the R_{V_i} are different. But we prefer to use the term ''homogeneous solution,'' bearing in mind that the slightly split solutions form a compact group. The second area ($U_V=18$ V–22 V, $1/R_C=0.2$ kΩ^{-1}–0.6 kΩ^{-1}) borders on two inhomogeneous stable steady states SS1 and SS2.

To produce additional DT modes, it is usually sufficient to make only one oscillator slightly different from its partners. Therefore, computations in the area near the boundary of the homogeneous steady state were performed for $R_{V_1}=3.92$ kΩ and $R_{V_{2,3}}=3.9$ kΩ; and in the area near SS1 and SS2 for $R_{V_1}=4.15$ kΩ and $R_{V_{2,3}}=3.9$ kΩ.

In the area near the boundary of the homogeneous steady state, solutions were found that existed only if two of the three oscillators were identical; therefore we examined the case when all three R_V values were different: $R_{V_1}=3.92$ kΩ, $R_{V_2}=3.9$ kΩ, and $R_{V_3}=3.89$ kΩ.

B. Evolution of basic modes in the presence of small detuning

All the basic modes are quite stable against relatively low noise and small detuning. However, the presence of detuning makes it necessary to refine the classification of those basic attractors in which there is no phase shift between two of the three oscillators. These solutions include the antiphase attractor 1/2 (one oscillator moves in antiphase with two others) and the inhomogeneous steady states. Let us consider, for example, the 1/2 limit cycle in which oscillators with indices 1 and 2 move in phase with each other and in antiphase with the third oscillator [Fig. 5(a)]. Specifically, we shall retard the first oscillator by varying R_{V_1}. When it begins to lag behind the second oscillator, the solution still resembles the antiphase solution. In fact, the lag between these oscillators is small, and their wave forms still remain identical [see Fig. 5(b)]. If the third oscillator is retarded, the other two continue to move in phase with each other, Fig. 5(c). Thus, small detuning splits the antiphase attractor into two other modes, which have different boundaries of stability in the phase diagram. In Fig. 6, these solutions are designated as 1/2 out (identical oscillators move in antiphase) and 1/2 in (in-phase oscillations of identical elements). Similar refinements can be made for the boundaries of steady state stability. However, in this case, the shifts in the phase point coordinates in the six-dimensional phase space are used, rather than the phase shifts between the oscillators, because they do not oscillate.

Along with splitting the boundaries of steady states and antiphase attractor stability, an expected result of detuning is the emergence of (i) quasiperiodical regimes and/or (ii) multiple synchronization, that is, long-period $i/j/k$-type regimes,

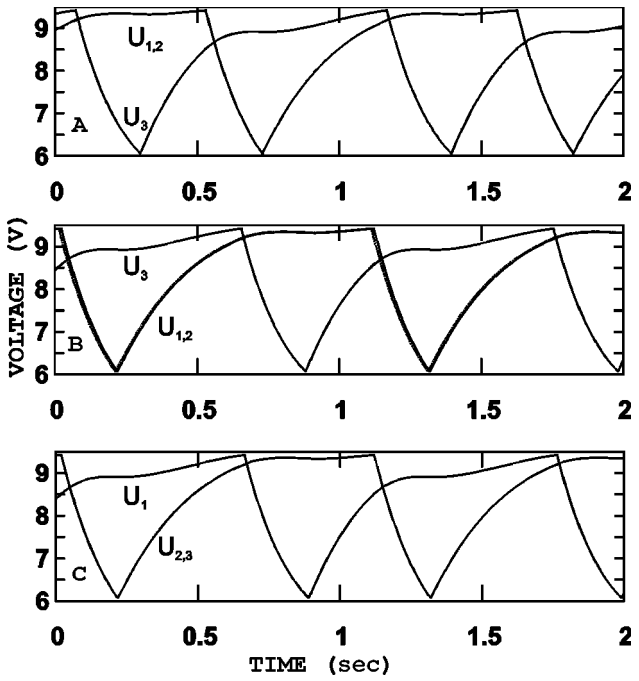

FIG. 5. Splitting of the antiphase limit cycle if one oscillator is slightly detuned. Parameters: $U_V=16$ V, $1/R_c=0.15$ kΩ^{-1}. (a) Initial solution for identical resistors $R_{V_1}=R_{V_2}=R_{V_3}=3.9$ kΩ; (b) and (c) two versions, 1/2 out and 1/2 in, of the antiphase limit cycle for $R_{V_1}=3.92$ kΩ, and $R_{V_2}=R_{V_3}=3.9$ kΩ.

with $i/j/k\gg 1$ being the numbers of oscillations performed by each oscillator in one full period. In both cases, the ISI distributions are narrow because of the smallness of detuning; therefore, we do not examine them. The wave forms of the in-phase (more precisely, almost in-phase) solution and of various rotating waves do not change in the presence of

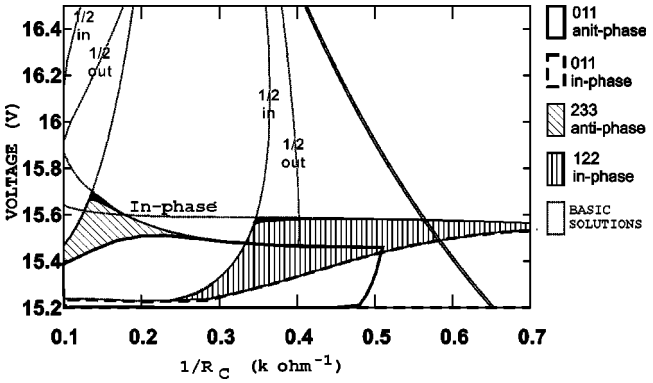

FIG. 6. Phase diagram of new modes for the system with one detuned oscillator at U_V near the Hopf bifurcation to the homogeneous steady state. The heavy thick line is the boundary of the inhomogeneous SS I. The in-phase regime is unstable below the dotted line marked with the ''In phase'' label; the dotted lines marked with the 1/2 in (out) labels are the boundaries between which the ''in'' and ''out'' antiphase regimes (see text for definition) are stable. The solid line bounds the region of stability of the 011 antiphase solution, which overlaps with the regions where the 011 in-phase (solid dashed line) and 122 in-phase regimes are stable. The small black triangular area that caps the region 2,3,3 antiphase is the region where the solution 4,5,5 antiphase is stable.

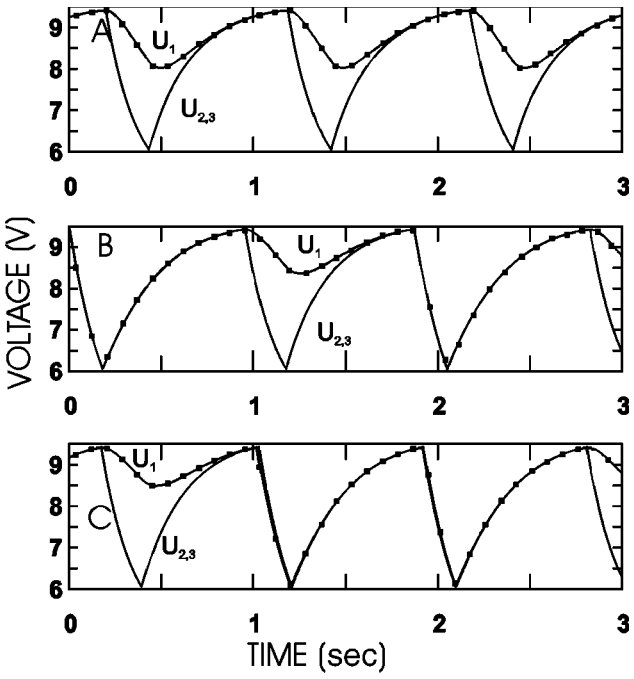

FIG. 7. Time series of slow variables for those solutions near homogeneous SSs (see Fig. 6) in which two identical oscillators move in phase: (a) in-phase DT (0,1,1 in phase) for $U_V=15.3$ V and $1/R_C=0.5$ kΩ^{-1}; (b) solution 1,2,2 in phase for $U_V=15.4$ V and $1/R_C=0.4$ kΩ^{-1}; and (c) solution 2,3,3 in phase for $U_V=15.58$ V and $1/R_C=0.35$ kΩ^{-1}. The time series of the detuned oscillator is marked by black squares.

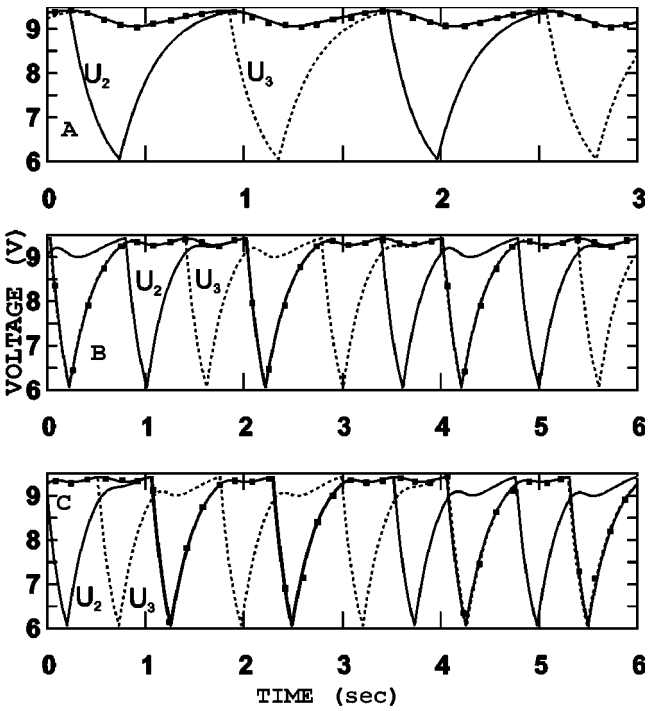

FIG. 8. Time series of slow variables for those solutions near homogeneous SSs in which two identical oscillators move in antiphase: (a) antiphase DT (0,1,1 antiphase) for $U_V=15.3$ V and $1/R_C=0.25$ kΩ^{-1}; (b) solution 2,3,3 antiphase for $U_V=15.5$ V and $1/R_C=0.15$ kΩ^{-1}; and (c) solution 4,5,5 antiphase for $U_V=15.68$ V and $1/R_C=0.14$ kΩ^{-1}. Black squares mark the time series of the first (detuned) oscillator.

detuning; however, the areas of existence of such solutions may shrink and/or be shifted in the phase diagram. The solutions discussed have been examined in detail in [26] and are presented here only for comparison with the new solutions described below.

C. Dynamic traps near the stable homogeneous steady state

As the oscillators are stiff and are selectively coupled by diffusion-driven exchange, small detuning disrupts the stability of the in-phase solution in the region $U_V\approx 15.2$ V. The boundary of the in-phase solution stability shifts up to $U_V\approx 15.6$ V, affording the possibility of formation of additional attractors (Fig. 6). Let us divide the solutions detected in this region into two groups and designate them as i,j,k in-phase and i,j,k antiphase, where i,j, and k are integers denoting the numbers of full-amplitude oscillations performed by individual oscillators in one period of the entire system (which is the smallest common multiple of their periods). The designation antiphase (in phase) means that the second and the third (identical) oscillators move in antiphase (phase). In each group, the solutions with different i,j,k do not coexist but share segments of the boundaries in common. Figures 7 and 8 depict the wave forms of the m,n,n in-phase and m,n,n antiphase solutions, respectively. As indicated in Sec. IV B, the basic antiphase solution can also appear in two forms now: $1/2$ in and $1/2$ out.

One can see in Fig. 6 that, when approaching the lower boundary $U_V=15.2$ V, the $1/2$ out solution transforms, depending on the coupling strength, into the 4,5,5 antiphase solution (if the oscillators are coupled weakly), into the 2,3,3 antiphase solution, or into the antiphase dynamic trap (the solution designated as 0,1,1 antiphase). As U_V decreases, the difference in the period between the first and the other two oscillators grows, because $T(U_V,R_V)$ is a nonlinear function (Fig. 4). However, at the lower U_V limit that we consider, the first oscillator is still detuned by no more than 3%.

The dynamic trap formation can be qualitatively explained as follows. If the period of one oscillator becomes even slightly longer than that of its partners, some critical rate of inhibitor exchange exists at which the detuned oscillator fails to reach the point of transition to the other branch of the nullcline. In other words, if the term $(U_2-2U_1+U_3)/R_C$ is almost always negative and close to $I_1-(U_V+U_1)/R_{V_1}$, the right-hand part of Eq. (2) for the slow unit oscillates around zero. This condition holds if the diffusion partners rapidly alternate, keeping the term $(U_2-2U_1+U_3)/R_C$ below zero. This makes clear why the area where the DT exists resides close to the boundary of limit cycle creation in the isolated oscillator and why this area expands with increasing coupling strength (Fig. 6). For rapid alternation of diffusion partners, it is required that oscillations of the units be highly asymmetrical and that the units be stiff, that is, capable of jumping fast from one branch of the nullcline to the other. Oscillation asymmetry is defined as the time ratio between the ascending and descending parts of the

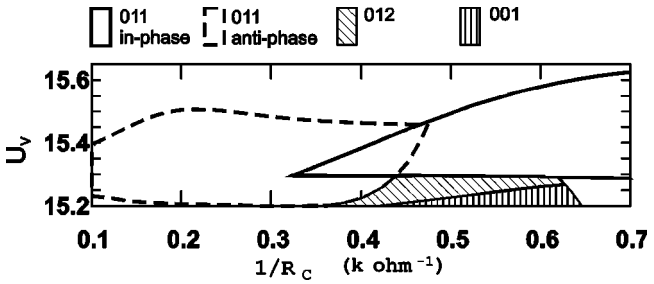

FIG. 9. Part of the phase diagram of the modes for the system in which all oscillators are slightly different: $R_{V_1}=3.92\ \mathrm{k}\Omega$, $R_{V_2}=3.9\mathrm{k}\Omega$ and $R_{V_3}=3.89\ \mathrm{k}\Omega$. Shadowed areas correspond to the additional DT types. See Fig. 10 below for their time series.

slow variable U wave forms of isolated oscillators. In the case under study, the oscillation is highly asymmetrical because the intersection point of the main nullclines is near one of the extrema of the N-shaped nullcline.

If the coupling strength is large, U exchange can so considerably retard one of the oscillators moving along the cycle that it becomes unable to reach the point of transition even if its neighbors oscillate in phase. In this way, an in-phase DT emerges [Fig. 7(a)]. For the in-phase DT to emerge, it is required that oscillations of isolated oscillators be asymmetrical. Highly asymmetrical oscillations imply that two oscillators almost instantly drop onto the right branch of the N-shaped nullcline, causing the detuned oscillator to reverse the direction of its movement. As the oscillators move along the left branch of the nullcline, the phase shift between them and the detuned oscillator diminishes until the latter stops receding and begins to move in the initial direction. However, this coupling-induced delay in its movement is so large that the second and third (identical) oscillators catch up with it and pass it when moving on the left branch to the point of transition, again reaching this point earlier. The process is then repeated.

Obviously, the period of the system is significantly shorter in this regime than in the antiphase DT because in the latter the inhibitory effect of the U exchange is pronounced on most of the limit cycle. With decreasing coupling strength, the in-phase DT jumps into the 1,2,2 in-phase regime, in which the first (detuned) unit skips every other full-amplitude oscillation of its neighbors [Fig. 7(b)]. As U_V increases, the 1,2,2 in-phase solution transforms into the 2,3,3 in-phase one [Fig. 7(c)] throughout the upper boundary, but the area where the 2,3,3 in-phase regime exists is very narrow.

It may seem that the 0,1,1 in-phase solution is degenerate and will lose stability if all three oscillators are set to be slightly different. However, the in-phase DT is stable against noise and exists even when the third oscillator moves more rapidly than the second. With highly detuned oscillators, the area of its existence is narrow. However, if the difference between the periods of the second and the third oscillators is 1–2%, this solution still occupies a large area in the parameter plane. Figure 9 shows the area of existence of the 0,1,1 in-phase solution for the case when all three oscillators are different with respect to R_{V_i} (as specified in the caption). The

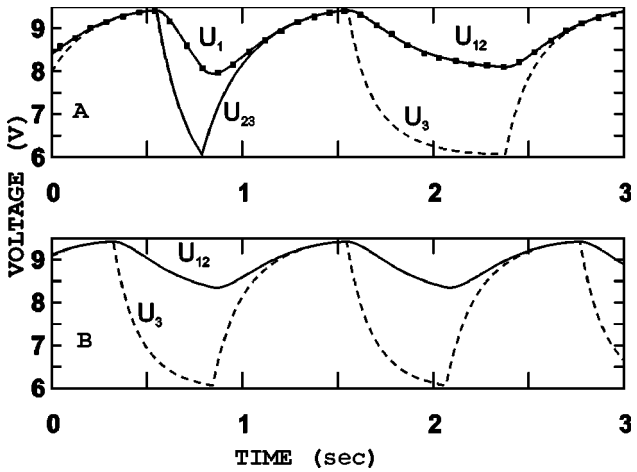

FIG. 10. Time series of slow variables U_i for the dynamical traps in the case when all oscillators are detuned near the homogeneous SS: (a) 0,1,2 DT for $U_V=15.275$ V and $1/R_C=0.6\ \mathrm{k}\Omega^{-1}$; and (b) 0,0,1 DT for $U_V=15.215$ V and $1/R_C=0.52\ \mathrm{k}\Omega^{-1}$. Squares mark U_1. The segments where the trajectories of the second and third or the first and second oscillators are almost indistinguishable are designated by $U_{2,3}$ or $U_{1,2}$, respectively.

additional nonidenticality gives rise to solutions of this and other types, including additional DTs. By way of example, we show the areas of existence of two DTs, the 0,1,2 and 0,0,1 in-phase DTs (Fig. 9).

If the coupling strength is sufficiently large and U_V is chosen near the boundary of the homogeneous SS, two slow oscillators may be synchronized over a segment of the trajectory close to the maximum of the N-shaped nullcline. This solution is similar to the 0,1,1 in-phase DT, but the faster oscillator in this case is the first to reach the point of transition, keeping the slower oscillators near this point. Obviously, the 0,0,1 solution is analogous to the 0,1,1 in-phase solution in the system with one detuned oscillator in the case when this oscillator is faster (rather than slower) than the others. The 0,1,2 solution is intermediate between the 0,0,1 in-phase and 0,1,1 in-phase DTs. As seen in Fig. 10(a), the wave form of this solution can be divided into two parts. The first part is specific in that the phase shift between the second and third oscillators is very small, as is typical of the in-phase 0,1,1 DT. The second part of the wave form is as in the 0,0,1 solution, because now the first and second oscillators move in phase.

V. DYNAMIC TRAPS NEAR STABLE INHOMOGENEOUS STEADY STATES

The mechanism examined above for suppressing full-amplitude oscillations is also likely to operate in the vicinity of the stable inhomogeneous SSs. As mentioned above in Sec. IV A, we search for DT solutions in this area of the parameter plane ($U_V=18$ V–22 V) for $R_{V_1}=4.15\ \mathrm{k}\Omega$ and $R_{V_2}=R_{V_3}=3.9\ \mathrm{k}\Omega$, which correspond to a few percent of difference in the the period between the first and the other two oscillators. In this area, the free oscillation period is a nonmonotonic function of U_V, with a minimum at U_V

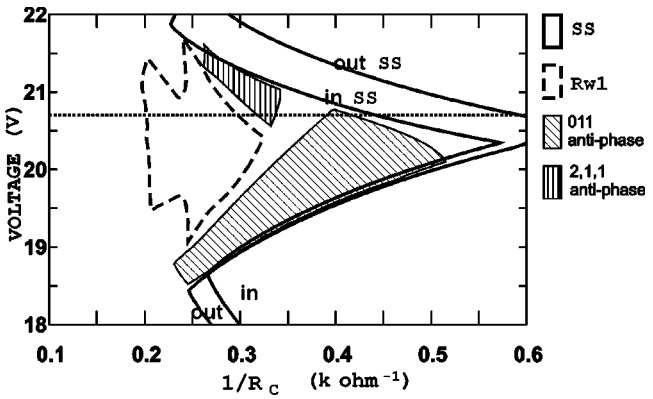

FIG. 11. Part of the phase diagram of the system with one oscillator slightly detuned near the inhomogeneous SS. The dotted line indicates U_V at which the free periods of all the oscillators are the same despite the fixed differences between their R_{V_i} values. See text for an explanation of the differences between the in and out SS.

$\approx$20.7 V for $R_V=3.9$ kΩ (dotted line in Fig. 11). Therefore, although the parameters R_{V_i} are fixed, the first oscillator turns out slower than the others at $U_V<20.7$ V and faster at $U_V>20.7$ V. With the bifurcation parameter $U_V\approx 20.7$ V, the free oscillation periods of the three oscillators are equal at the chosen R_{V_i} values, but the wave form shapes are slightly different.

Figure 11 shows two boundaries of the stable inhomogeneous SS. The boundary marked in SS corresponds to the solution in which the dynamic variables of the second oscillator coincide with those of the third one. The boundary marked out SS corresponds to the solution in which the *I* and *U* values of the first oscillator are close to those of the second or the third oscillator (for more detail see Sec. IV B, which describes splitting the SS and the antiphase attractor in the presence of detuning).

Comparing Figs. 3 and 11, one can see that, in the presence of even slight detuning, the area where the RW1 attractor exists becomes significantly smaller. In addition, its symmetry is broken, as judged from the distortion of the trajectory. Specifically, the wave forms of the slow variables of the symmetrical RW transform into the wave forms shown in Fig. 12(a). Evidently, the trajectory of the first (detuned) oscillator is elongated near the maximum of the N-shaped nullcline. This loss of symmetry is not associated, however, with any significant changes in the oscillation periods, because the delays described are compensated for in other segments of the trajectory, which are passed more rapidly.

Near the boundaries of the stable inhomogeneous SSs (but below $U_V\approx 20.7$ V), the possibility arises that the two oscillators moving in antiphase might keep the detuned oscillator short of the maximum of the N-shaped nullcline. In this way, a 0,1,1 antiphase DT emerges. A comparison of the wave forms of the slow variables of the antiphase DTs shown in Figs. 12(b) and 8(a) leads us to suggest that the reason why one of the oscillators is locked near the maximum of the nullcline is the same for both DTs, and that it lies in the alternate inhibitor influx. The DTs in the middle of the phase diagram are similar to the DT near the homogeneous SS in

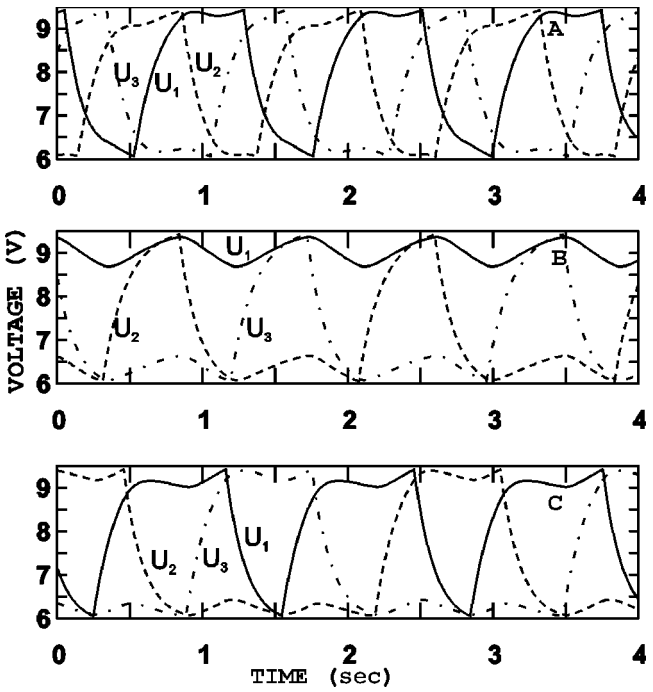

FIG. 12. Time series of slow variables U_i of the periodic solutions shown in the phase diagram (Fig. 11): (a) RW for $U_V=20$ V and $1/R_C=0.27$ kΩ^{-1}; (b) DT 0,1,1 antiphase for $U_V=19.5$ V and $1/R_C=0.32$ kΩ^{-1}; and (c) limit cycle 2,1,1 antiphase for $U_V=21$ V and $1/R_C=0.32$ kΩ^{-1}.

that the delays in the movement along the cycle are due to the formation of transient quasistationary states near the maximum of the nullcline. In both cases, it is the closeness to the SS, whether inhomogeneous or homogeneous, that makes their formation possible. Note that the emergence of DTs near the inhomogeneous SSs is feasible only if the partners of the detuned oscillator alternate sufficiently frequently. Being slightly retarded near the maximum of the nullcline, the first oscillator fails to reach the point of transition, remaining short of it.

One can see in Fig. 11 that the antiphase DT may be stable even if the first oscillator has a free period shorter than that of the others, because the line $U_V\approx 20.7$ V can cross the very limited area of existence of this solution so that a tiny part of it turns out to be slightly above this line. However, no contradiction arises with the explanation of this DT given above, because its stability is ensured by the properties of the local behavior of the first oscillator near the maximum of the N-shaped nullcline. Locally, near the maximum of the N-shaped nullcline, the first oscillator lags behind the two others despite the fact that their free periods are longer. In this case, the shorter free period of the first oscillator is accounted for by its fast movement when it passes through the minimum of the N-shaped nullcline. We detuned the first oscillator so that the point where the nullcline $U_1=R_{V_1}I_1-U_V$ intersects the N-shaped nullcline is closer to its maximum than the corresponding intersection points of the nullclines of the other oscillators. Therefore, near the maximum (minimum) of the nullcline, the first oscillator always moves more (less) slowly than the two others.

As seen in Fig. 11, with increasing coupling strength, the 0,1,1 antiphase solution transforms into out SS while coexisting with in SS. A similar phenomenon is observed near the homogeneous SS, where solutions from the same group (''antiphase'' or ''in phase'') share a common boundary (which implies no overlapping between them), while coexisting with the solutions from the other group. Above $U_V \approx 20.7$ V, it is natural to expect the appearance of $i, i-1, i-1$-type solutions, because the detuned oscillator is slightly accelerated in this area. The time series of the slow variables for the 2,1,1 antiphase limit cycle are presented in Fig. 12(b). Because oscillator 1 (fast) passes any of its partners when approaching the minimum of the N-shaped nullcline, the trajectories of oscillators 2 and 3 contain quasistationary segments. Just below $U_V \approx 20.7$ V, the 2,1,1 antiphase solution is also stable: the local situation near the minimum of the N-shaped nullcline is such that oscillator 1 again moves more rapidly than the others (see the discussion of the stability boundaries of the 0,1,1 antiphase DT.

Let us make a general remark about the sensitivity of the phase diagram structure to the specific way in which the electronic scheme is detuned. Although detuning is small, the way we set it is essential in the central region of the phase diagram. In this work, the same electronic scheme is considered as that in [26]. However, the detuning is set differently: R_{V_i} rather than capacitances (as in [26]) are varied. Comparing the phase diagrams (Figs. 13 and 14 in [26]) with those in Figs. 6 and 11 in this study, one can see that the areas near the homogeneous SSs are similarly rich in attractors, unlike the areas between the inhomogeneous SSs: the nonbasic attractors detected in this study were unobservable numerically in [26]. This discrepancy stems from the method of detuning and is accounted for by the insufficient coupling of the slower oscillator with its neighbors.

VI. EFFECTS OF EXTERNAL NOISE

To study the influence of fluctuations on the dynamics of the system (1), (2), uncorrelated samples of the normally distributed white noise $\xi_i(t)$ were added only to the right-hand sides of the slow variable equations (2). This additive noise is characterized by $\langle \xi_i(t) \rangle = 0$, $\langle \xi_i(t), \xi_j(t+\tau) \rangle = \sigma^2 \delta_{ij} \delta(\tau)$. When noise is present, we define the period as $T_i = t_{i+1} - t_i$, where t_i are the moments when the trajectory $U_i(t)$ crosses the chosen value of U_{cr} at the same sign of the derivative. The T_n's defined in this way usually coincide with the time intervals between two consecutive bursts of the fast variable. As with the DT, the area near the homogeneous SS is most promising from the standpoint of revealing nontrivial noise-induced dynamic effects, even in the case of identical oscillators. The ISI distributions typical of this area ($U_V \approx 15.2$ V) are shown in Fig. 13 for different coupling strengths.

As seen in this figure, the effect of noise does not come down to a mere broadening of the peaks of the ISI distributions, which correspond to the periods of stable limit cycles. With the identical oscillators that we consider, only the in-phase limit cycle is stable in this part of the parameter plane for R_c^{-1} in the interval 0.4–0.6 $\mathrm{k}\Omega^{-1}$. Nevertheless, noise

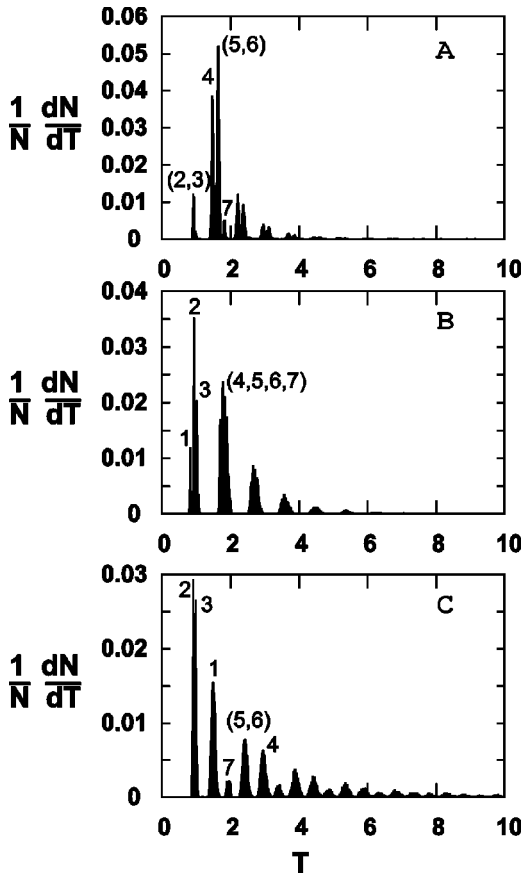

FIG. 13. ISI distributions in the system of identical oscillators near the Hopf bifurcation in the presence of uncorrelated noise for different coupling strengths: (a) $1/R_C = 0.2$ $\mathrm{k}\Omega^{-1}$ and $N = 31\,452$; (b) $1/R_C = 0.35$ $\mathrm{k}\Omega^{-1}$ and $N = 38\,099$; and (c) $1/R_C = 0.6$ $\mathrm{k}\Omega^{-1}$ and $N = 36\,440$. General parameters: $U_V = 15.3$ V and $\sigma = 0.001$. N is the number of ISIs computed for a given distribution. For convenience of microscopic analysis, the peaks are enumerated. Their numbers are used in Sec. VI to indicate which parts of the trajectories contain the corresponding periods.

not only broadens the ISI peak corresponding to the period of the in-phase solution, but also gives rise to a discrete spectrum of ISIs with decreasing peak amplitudes. The discretization effect of noise depends only slightly on its amplitude and is observed up to $\sigma = 10^{-5}$. However, as the system moves farther away from the boundary of the homogeneous SS (that is, with increasing U_V), the peaks tend to vanish. Obviously, as the oscillations are highly asymmetrical, the oscillators spent much time near the point of transition on the left branch of the N-shaped nullcline. This area in the vicinity of the nullcline maximum is most vulnerable to noise. Away from the boundary of the homogeneous SS, the oscillations become less asymmetrical, accounting for the attenuation of the effects of noise.

To gain more insight into the nature of the peaks in the ISI distributions shown in Fig. 13, fragments of the slow variable wave forms that contain the ISIs contributing to these peaks are presented in Fig. 14 ($1/R_C = 0.35$ $\mathrm{k}\Omega^{-1}$) and Fig. 15 ($1/R_C = 0.2$ $\mathrm{k}\Omega^{-1}$).

Let the oscillators be enumerated in the chain and let us

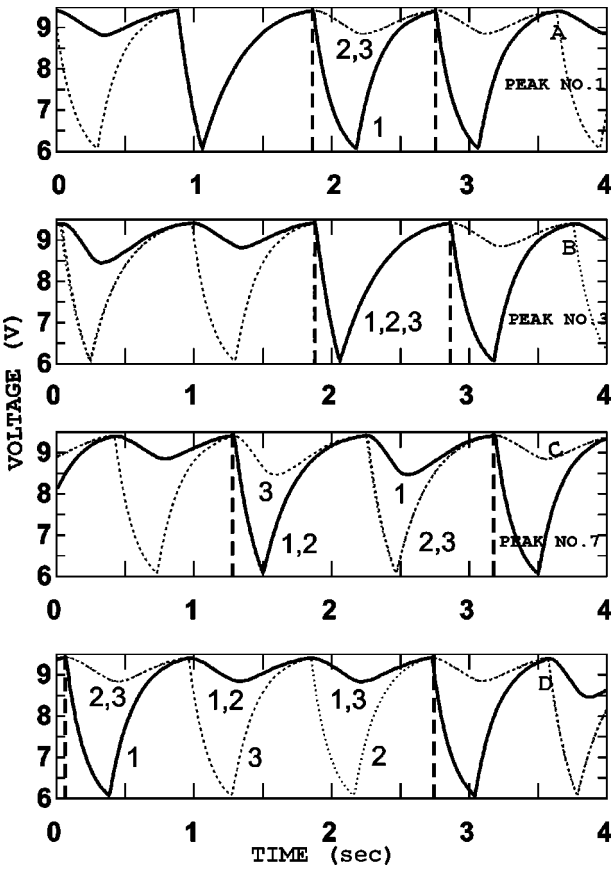

FIG. 14. Time series of slow variables U_i of the system of identical oscillators in the presence of noise. Parameters $U_V = 15.3$ V, $1/R_C = 0.35$ kΩ^{-1}, $\sigma = 0.001$ are as in Fig. 13(b). The solid line in bold shows the trajectory of oscillator 1. The moments of two consecutive bursts of oscillator 1 are indicated by vertical dashed lines.

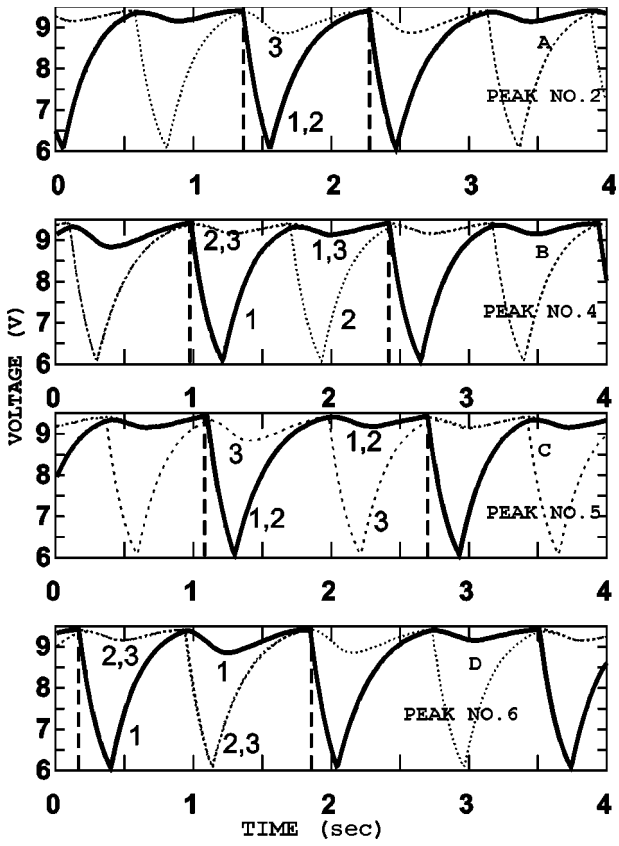

FIG. 15. The same as in Fig. 14 but for $1/R_C = 0.2$ kΩ^{-1}.

consider their most likely trajectories in between the spikes produced by the first oscillator. For convenience, the moments of firing of the first oscillator are marked with vertical dashed lines (in bold) and its trajectory is shown with a thick solid line (Figs. 14 and 15). Each of the trajectories considered below is designated with the same number as that used to mark the peak in the ISI distribution shown in Fig. 13 to which the periods contained in that trajectory contribute.

(1) Let us start with Fig. 14(a). In this noise sample, oscillator 1 is the first to jump from the slow left branch of the N-shaped nullcline. After its jump, coupling causes the other oscillators to stop advancing to the point of transition and to perform a trip along a small loop near the nullcline maximum. This loop in the phase portrait corresponds to the deflection in the wave form. Completing the cycle, the first oscillator begins to approach its partners. At this stage of the cycle, coupling reduces the phase shifts between the oscillators. In the presence of this particular sample of noise, the first oscillator is again the first to jump despite the delay in its movement. For this event to occur, the lag between the first and the other two oscillators when they come close to the point of transition has to be less than the boosting effect of noise on the first oscillator; therefore, the higher the noise amplitude and the greater the coupling strength, the higher the probability of the trajectory described. If the coupling strength is insufficient, this pattern is unobservable [see Fig. 13(a), $1/R_C = 0.2$ kΩ^{-1}]. With increasing coupling strength, its probability grows, and the peak corresponding to this pattern arises in the ISI distributions [Fig. 13(b), $1/R_C = 0.35$ kΩ^{-1}, peak no. 1]. As the coupling strength increases further [see Fig. 13(c), $1/R_C = 0.6$ kΩ^{-1}], the peak area enlarges (and, hence, the probability of the event becomes higher). In addition, the mean time required for the oscillator to make a trip along the trajectory described (let us denote it T_1) also increases with the coupling strength, which shifts the peak to longer T values.

(2) Oscillators 1 and 2 jump from the slow left branch of the N-shaped nullcline [Fig. 15(a)]. This event causes oscillator 3 to perform a trip along a small loop near the nullcline maximum. On completing the cycle, the oscillators are close to one another, but oscillators 1 and 2 are somewhat farther from the maximum than oscillator 3. Nevertheless, this particular sample of noise is such that oscillator 1 surpasses oscillator 3 and is the first to jump. Along the trajectory considered, the equation for $U_3(t)$ includes the coupling term $(U_1 - 2U_3 + U_2)/R_C \approx 2(U_1 - U_3)/R_C$, because $U_2 \approx U_1$. In the previous case, this term was $\approx (U_1 - U_3)/R_C$, because $U_3 \approx U_2$.

Hence, it is certain that, when the oscillators approach the point of transition, the gap between the leading oscillator 3 and the lagging oscillators 1 and 2 is shorter on this trajectory than the gap between the leading oscillator 1 and the lagging oscillators 2 and 3 on the previous trajectory de-

scribed in paragraph 1. Therefore, significantly lower coupling strengths are sufficient to observe this trajectory. Compared with T_1, T_2, which is the mean time required for the oscillator to perform the described trip, depends on the coupling strength to a lesser extent. This is understandable, because the coupling term for oscillator 1 (which we monitor) is either $\approx(U_3-U_1)/R_C$ when it follows the T_2 trajectory, where $U_1\approx U_2$; or $\approx 2(U_3-U_1)/R_C$ when it follows the T_1 trajectory, where $U_2\approx U_3$. As seen in Fig. 13, no noticeable shift in the peak 2 position could be obtained by varying the coupling strength.

(3) In Fig. 14(b), all three oscillators simultaneously jump from the slow left branch of the nullcline and move together up to the next transition point, where oscillator 1 jumps again. Being unaffected by coupling, the mean time it takes an oscillator to run this trajectory (T_3) is equal to the period of the in-phase limit cycle in the noise-free system. However, the probability of such an event depends on the phase shifts between the oscillators near the transition points. The higher the coupling strength, the smaller the phase shifts, and the more probable the noise-induced in-phase trip. As expected, the peak 3 amplitude, which is the lowest in Fig. 13(a), increases in 13(b), and further increases in 13(c).

(4) In the sections below, we explain why the period of oscillator 1 may become longer and longer. First, let it jump from the left slow part of the nullcline [Fig. 15(c)], causing its partners to move together along the small-loop-containing trajectory. Initially, the oscillators move along this trajectory as in the case shown in Fig. 1, but, when they approach the next transition point, a random gate opens only for oscillator 2. It jumps, forcibly retarding oscillators 1 and 3 by the time required for running the loop. Near the next transition point, oscillator 1 gets a chance to be the first to fire. As seen in Fig. 15(b), the trajectory considered consists of two parts. The second part is essentially the same as the first one, only with oscillator 1 in place of oscillator 2. Therefore, the time required for oscillator 1 to complete the trajectory averages $T_4\approx T_1+T_1$ [compare the positions of peaks 4 and 1 in Figs. 13(b) and 13(c)]. The higher the probability that oscillator 1 will jump when approaching the point of transition, the higher the probability of observing trajectory 1 and, correspondingly, the lower the probability of finding trajectory 4 among noise-induced time series.

(5) Oscillators 1 and 2 jump from the slow part of the nullcline, and coupling causes oscillator 3 to make a trip along the small loop [Fig. 15(c)]. Until the next maximum, trajectory 5 is as in case 2. However, the noise sample in this case is such that it is oscillator 3, rather than oscillator 1, that is the first to jump. After its jump, coupling sends oscillators 1 and 2 along the small loop in the phase plane. Meanwhile, oscillator 3 moves along the main path and again approaches the point of transition, lagging somewhat behind oscillators 1 and 2. Oscillator 1 jumps earlier than oscillator 3. Like the trajectory corresponding to peak 4, this trajectory consists of two parts: $T_5\approx T_2+T_1$. As in case 4, the higher the probability of observing trajectory 2, the lower the probability of finding trajectory 5 in the noise-induced time series.

(6) The trajectory presented in Fig. 15(d) is in essence trajectory 5, in which the internal components are arranged in the reverse order. It means that $T_6\approx T_1+T_2$, $T_6\approx T_5$. These periods contribute to the same peak of the ISI distributions.

(7) Yet another trajectory that contains only one loop-associated delay of oscillator 1 is presented in Fig. 14(c). With this noise sample, a series of two jumps is observed. Each time, two oscillators jump together, first oscillators 1 and 2 and then oscillators 2 and 3. The mean period $T_7\approx T_2+T_2$, as clearly seen in Fig.13(c).

(8) The peaks in Fig. 13 are relatively regularly spaced, suggesting that the solutions giving rise to this spectrum are such that, until firing, an oscillator performs several trips along the small loop. In fact, the reasoning presented above [(4)–(7)] can easily be extended to general cases with any number of trips. We confine ourselves to considering the simplest trajectory, which is presented in Fig. 14(d). Obviously, the mean period equals $3T_1$, because the trajectory consists of three components, each of which can be treated like the trajectory described in paragraph 1 (after changing oscillator numbering).

Thus, a detailed analysis of the dynamics can explain why the ISIs are so variable if three identical relaxation oscillators are coupled via U exchange. The results presented, while being relevant to stiff systems, do not change qualitatively with the stiffness. Variation in the voltage supply U_V or in the coupling strength also changes them only quantitatively. There exist R_C and U_V intervals where the discretization effect is most pronounced, e.g., near the homogeneous SSs. In other areas of the phase diagram ($U_V\in(16–17)$ V), where two or three basic limit cycles coexist, the ISI distributions usually contain two or three peaks (see [22]). However, this polymodality is less striking than that induced by noise in the ring of identical oscillators moving along the unique in-phase attractor [Figs. 13(b) and 13(c)].

The position of peak 3 (in phase) in the ISI distributions is independent of the coupling strength, unlike other peak positions, which vary differently with its increase. Peak splitting is clearly seen in Fig. 13(b); however, this event is not frequent. As $1/R_C$ is about 0.35 $k\Omega^{-1}$, peak 1 is close to peak 2 [Fig. 13(b)], giving rise to relatively broad unresolved peaks in this figure, in which the interpeak spacings are the largest. This means that the ISI distributions should be investigated in a broad range of coupling strengths to be sure that the essential dynamic processes will not be masked by overlapping and will manifest themselves in the ISI distributions.

A parallel may be drawn between abnormal ISI variability and the sets of attractors described in Secs. III and IV. Formally, the definition of deterministic attractors is valid only in the absence of noise. However, for relaxation oscillations in the chosen area of the parameter plane, the effect of noise is restricted to quite a small part of the trajectory in the vicinity of the maximum of the N-shaped nullcline. Noise causes only short-term variations in the parameters. Therefore, the basic ISI peaks can be brought into qualitative correspondence with the attractors detected in the system of weakly detuned oscillators (see Sec. IV) and specifically related to detuning. For example, peaks 1, 2, and 3 correspond to the 0,0,1 DT, 0,1,1 in-phase, and in-phase solutions, respectively.

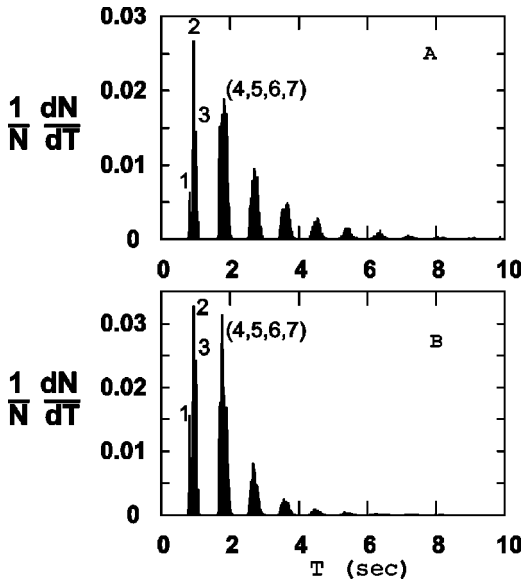

FIG. 16. (a) ISI distribution for the detuned oscillator ($N=12\,281$); and (b) ISI distribution for the other two oscillators ($N=33\,078$). Parameters: $U_V=15.3$ V, $1/R_C=0.35$ kΩ^{-1}, $\sigma=0.001$, $R_{V_1}=3.92$ kΩ, and $R_{V_2}=R_{V_3}=3.9$ kΩ.

As mentioned above (Sec. IV), the basic in-phase solution, which is unique in certain regions near the homogeneous SS, becomes unstable in the presence of small detuning. In these parameter regions, in-phase oscillations of identical units are easily disrupted in the presence of noise [see, e.g., Fig. 14(b)]. Both phenomena have the same nature: the slow variable exchange between stiff oscillators.

The permanent presence of small detuning should change the noise-induced ISI distributions. The retardation of one oscillator often gives rise to multiloop long-period trajectories. This effect for a ring with one retarded oscillator is illustrated in Fig. 16. To compare the ISI distributions, we set $1/R_C=0.35$ kΩ^{-1}, as in Fig. 13(b) for identical oscillators. The distributions are pictured separately for the first oscillator [Fig. 16(a)] and the two others [Fig. 16(b)]. As expected, the detuned oscillator is more likely to have long ISIs, as compared with its partners, but qualitative differences between the distributions in Figs. 16 and 13(b) are difficult to find; namely, the ISI distribution shape, the degree of intrapeak splitting, and the mean interpeak spacing remain almost unchanged.

Hence, with reasonable values of noise amplitudes and detuning, the latter produces no qualitative changes in the dynamic behavior of the oscillator ring.

In the middle of the phase diagram (near the boundaries of the inhomogeneous SSs), no noise-induced polymodality of the ISI distributions can be observed even in the presence of detuning, which gives rise to additional attractors. All the basic solutions in this region remain stable against low-amplitude noise. An increase in the noise amplitude breaks down these solutions, and the system settles onto the in-phase attractor, which has the largest basin in this area of the parameter plane.

The sensitivity of the present solutions to noise varies in a broad range, but formally, like the basic ones, they are all stable against noise. The results of numerical experiments designed to determine the effect of noise on the mean lifetime of various solutions in a system of nonidentical oscillators are presented in Table I. The 0,1,1 antiphase DT is observable if the noise amplitude σ is lower than 0.008. The RW is absolutely insensitive to the noise in this amplitude range, whereas the 2,1,1 limit cycle persists if σ is lower than 0.0008 and is immediately and completely broken down at larger noise amplitudes.

Therefore, with properly chosen initial points, the detuning-related nontrivial solutions in the vicinity of the inhomogeneous SSs are quite observable in the presence of controlled noise. However, they do not manifest themselves spontaneously in the ISI spectra, as they do in the vicinity of the homogeneous SS, because of the dominance of the in-phase solution.

VII. DISCUSSION

Comprehensive studies of systems of several more or less identical oscillators have revealed the mechanisms whereby

TABLE I. Mean lifetimes (s) of the solutions near the boundary of the inhomogeneous SSs in a system of nonidentical oscillators for various noise amplitudes (σ). The parameters used in the computations are the same as those in Fig. 11 (phase diagram). Number of random trials used to obtain the mean is given in parentheses. If no decay of the solution was detected over time X (s), its lifetime is written as "$>X$."

Solution, values of parameters	$\sigma=0.01$	$\sigma=0.008$	$\sigma=0.005$	$\sigma=0.003$	$\sigma=0.001$	$\sigma=0.0008$
0,1,1 antiphase, $U_V=19.5$ V $1/R_C=0.35$ kΩ^{-1}	6.0 (216)	9.4 (294)	>185	>187	>189	
2,1,1 antiphase, $U_V=21.0$ V $1/R_C=0.31$ kΩ^{-1}	1.5 (224)	1.7 (258)	2.0 (255)	3.0 (250)	27.0 (36)	>153
RW1, $U_V=20.5$ V $1/R_C=0.25$ kΩ^{-1}	>336	>335				

rhythms are generated ([3,8,16,9,18,21,27]). As shown recently, multiple phase-locked states are typical of delay-coupled limit-cycle oscillators [30]. Among them, the most expected are antiphase oscillations and rotating waves. If several attractors coexist in the same region of the parameter space, noise can induce infinite transitions between the attractors. Therefore, in the presence of noise, the ISI distributions are expected to contain not only peaks corresponding to the oscillation periods of the attractors, but also peaks corresponding to the characteristic times of transitions between the attractors. However, in the largest part of the areas where the basic attractors coexist, the maximum ISI distribution widths are determined by the attractor period ratio and are relatively small.

In our opinion, slow variable exchange between relaxation oscillators is a powerful mechanism for generating rhythms. For convenience, two-dimensional oscillators are usually studied, although they not always adequately correspond to real processes. In such systems, additional stable limit cycles occupy large regions in the parameter space and have large basins of attraction. In addition, stiff systems are easy to govern by externally varying the parameters or phase variables, because it is typical of such systems that they quickly settle on the attractors and rapidly switch between them. With an increase in the number of oscillators, the phase space volume rises less rapidly than the number of stable attractors. As a result, the so-called crowding of attractors is observed [31]. In its turn, crowding enhances the effect of noise on the dynamics of the system.

In a previous study [26], periodic regimes were examined in the presence of small stationary detuning, which proved to be an important bifurcation parameter. In this study, we focused on the analysis of complex patterns of ISI distributions generated by uncorrelated noise in various regions of the parameter space in the presence or in the absence of small detuning. In addition to the basic periodic attractors (see Sec. IV), coupling via slow variable exchange gives rise to a variety of unexpected attractors. If the relaxation parameter is in a reasonable range ($\varepsilon \sim 0.1$), slow variable exchange affords stability to DTs in a broad range of coupling strengths, but only near the boundary of creation of limit cycles of isolated oscillators [28]. As the relaxation parameter increases, the range of DT stability shrinks. However, DTs are readily generated in the presence of even small detuning (see Sec. IV C). Comprehensive analysis of the wave forms of one oscillator in a ring of identical oscillators (Sec. VI) reveals that long ISIs often result from randomly created more or less long elements of the DT. As the segments of the trajectory where relaxation oscillators are sensitive to noise are quite small (only in the close vicinity of the nullcline extrema), noise can be interpreted as a source of short-lived detuning, which delays one or two of the moving oscillators. Importantly, in the area near the Hopf bifurcation ($U_V \approx 15.2$ V in our system) where the in-phase limit cycle is formally stable, its attraction is weak, and it is a poor competitor against other randomly generated trajectories.

The situation is different near the inhomogeneous Hopf bifurcation ($U_V = 18$ V–22 V). In this region of the parameter space, small detuning also gives rise to different regimes, but it almost does not affect the basin of attraction of the in-phase regime. Therefore, it depends on the way in which the system is detuned whether the DT is observable or not (see Sec. V).

Thus, abnormally broad ISI distributions are quite possible for a system of three identical and simple (two-dimensional) limit cycles coupled via slow variable exchange. Such distributions are observed in large but specially selected regions of the parameter space. It is evident from the microscopic analysis (Sec. VI) that the phenomenon described may be observed not just for three oscillators.

The ISI distribution presented, for example, in Fig. 13(b) closely resembles the distribution obtained in studies of stochastic resonance (SR) (see, for example, [32]). With classic SR, the sensitivity of the system to noise is modulated by an external periodic signal. Our model is distinct in that the sensitivity to noise is modulated by slow variable exchange, and the mean ISI is determined by the relaxation time of the slow variable. As no external periodic signal acts on our system, we cannot speak about SR, but we can expect ''autonomous'' SR (or, according to [34], ''coherence resonance'') to manifest itself [33], because a change in the noise level modulates the degree of ISI coherence. Work on this is in progress.

In conclusion, it may be said that generation of abnormal fluctuations in systems of coupled oscillators is not restricted to systems with local diffusion. Very recently, a study of globally coupled systems appeared that describes large desynchronizing effects of low-level noise [35].

ACKNOWLEDGMENT

This work was supported by the Russian Foundation of Basic Research.

[1] A.T. Winfree, J. Theor. Biol. **16**, 15 (1967).
[2] T. Pavlidis, J. Theor. Biol. **33**, 319 (1971).
[3] M. Kawato and R. Suzuki, J. Theor. Biol. **86**, 547 (1980).
[4] D.A. Linkens, Bull. Math. Biol. **39**, 359 (1977).
[5] H. Yuasa and M. Ito, Biol. Cybern. **63**, 177 (1990).
[6] J.J. Collins and I. Stewart, Biol. Cybern. **68**, 287 (1993).
[7] M. Golubitsky, I. Stewart, P.-L. Buono, and J.J. Collins, Physica D **115**, 56 (1998).
[8] R.H. Rand and P.J. Holmes, Int. J. Non-Linear Mech. **15**, 387 (1980).
[9] D.G. Aronson, E.J. Doedel, and H.G. Othmer, Physica D **25**, 20 (1987).
[10] P. Ashwin, G.P. King, and J.W. Swift, Nonlinearity **3**, 585 (1990).
[11] A. Sherman and J. Rinzel, Proc. Natl. Acad. Sci. U.S.A. **89**, 2471 (1992).
[12] R.C. Elson *et al.*, Phys. Rev. Lett. **81**, 5692 (1998).
[13] J.N. Blakely *et al.*, Chaos **10**, 738 (2000).
[14] D. Ruwisch *et al.*, Phys. Lett. A **186**, 137 (1994).
[15] M. Marek and I. Stuchl, Biophys. Chem. **3**, 241 (1975).

[16] I. Schreiber, M. Holodniok, M. Kubiček, and M. Marek, J. Stat. Phys. **43**, 314 (1986).
[17] K. Bar-Eli, J. Phys. Chem. **94**, 2368 (1990).
[18] M.F. Crowley and I.R. Epstein, J. Phys. Chem. **93**, 2496 (1989).
[19] M. Yoshimoto, K. Yoshikawa, and Y. Mori, Phys. Rev. E **47**, 864 (1993).
[20] N. Nishiyama, Physica D **80**, 181 (1995).
[21] E.I. Volkov and M.N. Stolyarov, Phys. Lett. A **159**, 61 (1991).
[22] E.I. Volkov and M.N. Stolyarov, Biol. Cybern. **71**, 451 (1994).
[23] J. Gerhart, M. Wu, and M. Kirschner, J. Cell Biol. **98**, 1247 (1986); A. Goldbeter, G. Dupont, and M. Berridge, Proc. Natl. Acad. Sci. U.S.A. **87**, 1461 (1990); J. Das and H.-G. Busse, Biophys. J. **60**, 369 (1991).
[24] V.A. Vasiliev, Ju.M. Romanovskii, and V.G. Yahno, Sov. Phys. Usp. **22**, 615 (1979).
[25] D. Somers and N. Kopell, Biol. Cybern. **68**, 393 (1993); Physica D **89**, 169 (1995).
[26] D. Ruwisch, M. Bode, D.V. Volkov, and E.I. Volkov, Int. J. Bifurcation Chaos Appl. Sci. Eng., **9**, 1969 (1999).
[27] G.S. Cymbalyuk, E.V. Nikolaev, and R.M. Borisyuk, Biol. Cybern. **71**, 153 (1994).
[28] E.I. Volkov, Biofizika **43**, 535 (1998) [Biophysics (Engl. Transl.) **43**, 505 (1998)].
[29] E.I. Volkov and D.V. Volkov, Kratk. Soobshch. Fiz. 4, 25 (1998) [Bull. Lebedev Phys. Inst. **4**, 25 (1998)].
[30] D.V. Ramana Reddy, A. Sen, and G.L. Johnston, Phys. Rev. Lett. **80**, 5109 (1998); **85**, 3381 (2000).
[31] K. Wiesenfeld and P. Hadley, Phys. Rev. Lett. **62**, 1335 (1989).
[32] Proceedings of the NATO Advanced Research Workshop on Stochastic Resonance in Physics and Biology, edited by F. Moss, A. Bulsara, and M.F. Shlesinger [J. Stat. Phys. **70**, 1 (1993)].
[33] A. Longtin, Phys. Rev. E **55**, 868 (1997).
[34] A.S. Pikovsky and J. Kurths, Phys. Rev. Lett. **78**, 775 (1997).
[35] J. Teramae and Y. Kuramoto, Phys. Rev. E **63**, 036210 (2000).